

Farnesol-induced apoptosis in oral squamous carcinoma cells is mediated by MRP1 extrusion and depletion of intracellular glutathione

Chaidan Intapa^{1,2}, John Basile¹ and Mary Ann Jabra-Rizk^{1,3,*}

¹Department of Oncology and Diagnostic Sciences, University of Maryland, Baltimore, USA.

²Department of Oral Diagnosis, Faculty of Dentistry, Naresuan University, Thailand.

³Departments of Microbiology and Immunology, School of Medicine, University of Maryland, Baltimore, USA.

ABSTRACT

Farnesol is a key intermediate in the sterol biosynthesis pathway in eukaryotic cells that has exhibited significant anti-cancer and antimicrobial activity. We have shown that farnesol triggers apoptosis in oral squamous carcinoma cells (OSCCs) via a classical apoptotic process. However, the exact mechanism of farnesol cytotoxicity in eukaryotic cells has not been fully elucidated. In the cell, hydrophobic xenobiotics conjugate with glutathione, an antioxidant crucial for cellular detoxification against damaging compounds. This process results in the formation of glutathione S-conjugates which act as substrates for export by ATP-binding cassette (ABC) transporters and are extruded from the cell. This study was undertaken to validate the hypothesis that farnesol conjugation with intracellular glutathione coupled with multidrug resistance-associated protein 1 (MRP1)-mediated extrusion of glutathione-farnesol conjugates and oxidized glutathione results in total glutathione depletion, oxidative stress and ultimately cell death. The combined findings demonstrated that farnesol

exposure resulted in significant decrease in intracellular glutathione levels concomitant with decrease in cell viability. However, the exogenous glutathione maintained intracellular levels and enhanced viability. Furthermore, gene and protein expression studies demonstrated significant and rapid up-regulation of MRP1 in cells treated with farnesol. However, MRP1 blocking and transfection with a monoclonal antibody enhanced cell tolerance to farnesol. This is the first study describing the involvement of MRP1-mediated glutathione efflux as a mechanism for farnesol-induced apoptosis in cancer cells. Understanding of the mechanisms underlying farnesol-cytotoxicity may lead to the development of this redox-cycling agent as an alternative chemotherapeutic target.

KEYWORDS: oral squamous carcinoma, apoptosis, farnesol, glutathione, MRP1

ABBREVIATIONS

OSCCs: Oral squamous carcinoma cells; MRP1: Multidrug resistance-associated protein 1; GSH: Glutathione; GSSG: Glutathione disulfide; ABCT: ATP-binding cassette superfamily of transporters.

INTRODUCTION

Apoptosis, or programmed cell death, is a gene-controlled, tightly regulated process, which occurs naturally to restrict the proliferation of undesired

*Corresponding author: Mary Ann Jabra-Rizk,
Department of Oncology and Diagnostic Sciences,
University of Maryland, Dental School,
650 W Baltimore Street, 7 N, Room 2753,
Baltimore, MD 21201, USA.
mrizk@umaryland.edu

cells [1, 2]. The inhibition or de-regulation of this process, combined with altered cell proliferation, provides the basis for many cancerous diseases such as oral squamous cell carcinoma (OSCC), which accounts for more than 90% of head and neck cancers [3]. In mammalian cells, apoptotic cell death can be triggered by many different extracellular and intracellular stimuli resulting in the activation of extrinsic and intrinsic apoptotic signaling pathways [4, 5]. Among the recently identified extracellular stimuli of apoptosis in human tumor cells is farnesol, a naturally available sesquiterpene alcohol and a key intermediate in *de novo* synthesis of sterol in eukaryotic cells [6-10].

Our earlier work had demonstrated that farnesol promotes apoptosis in oral squamous carcinoma cells (OSCCs) via both the intrinsic and extrinsic apoptotic signaling pathways involving mitochondrial degradation, reactive oxygen species (ROS) accumulation, decrease in survivin and activation of intracellular caspases [4, 11]. Further, through global proteomic analysis of farnesol-treated cells, our findings revealed significant up-regulation of proteins involved in the inhibition of carcinogenesis, proliferation suppression and aging [11]. Earlier studies by others investigating the apoptotic effects of farnesol on certain human tumor cells demonstrated that farnesol resulted in the rapid inhibition of phosphatidylcholine synthesis, the most abundant lipid present in eukaryotic cell membranes [1]. It was concluded from these observations that farnesol-induced apoptosis is likely due to inhibition of the protein kinase C activator diacylglycerol required for cell proliferation [9]. However, the exact underlying mechanism of farnesol cytotoxicity in eukaryotic cells has yet to be fully elucidated. Since oxidative stress and apoptosis have been reported to be associated with intracellular glutathione depletion, we investigated the impact of farnesol on glutathione as an alternate pathway involved in the mechanism behind farnesol cytotoxicity.

Glutathione, present mainly in its reduced form (GSH), is a ubiquitous thiol-containing tripeptide composed of cysteine, glutamic acid and glycine, synthesized in the cell by the sequential actions of a series of six-enzyme-catalyzed reactions termed

the γ -glutamyl cycle [12-16]. Glutathione plays a key role in cellular resistance against oxidative damage through the detoxification of free radicals and naturally occurring deleterious compounds, as well as a variety of xenobiotics [12, 13, 15, 17]. Therefore, the response of a cell to stress involves changes in glutathione content, which is consumed in reactions that protect the cell by removing damaging compounds [12].

Glutathione detoxifies xenobiotics and toxic compounds through irreversible conjugation, concomitant with its conversion to the oxidized form, a reaction catalyzed by glutathione peroxidase (GPX). This reaction results in the formation of glutathione S-conjugates which are ultimately excreted from the cell [12, 13, 16]. The oxidized form, glutathione disulfide (GSSG), normally represents less than two percent of the total glutathione pool with the reduced GSH predominating over GSSG [13, 15]. Perturbations of the GSH/GSSG ratio can affect the redox status and induce cellular apoptosis and thus the ratio is regulated tightly to maintain cellular homeostasis [13, 15]. Therefore, the intracellular content of GSH is a function of the balance between depletion and synthesis [13, 15]. Cells use two competing mechanisms to maintain low levels of GSSG and high intracellular ratios of GSH to GSSG. The first mechanism is a recycling reaction where GSSG is reverted to GSH by the action of the enzyme glutathione reductase (GLR), which rapidly converts GSSG to GSH. The second mechanism involves cellular export of GSSG by membrane efflux pumps [12, 13, 17].

In mammalian cells, the release of glutathione S-conjugates from cells is an ATP-dependent process mediated by integral plasma membrane glycoproteins, the multidrug resistance proteins (MRP), belonging to the ubiquitous ATP-binding cassette superfamily of transporters (ABCT) [18, 19]. MRP1 plays a major role in conferring drug resistance as well as protecting normal tissues from cytotoxic drugs. The ABC transporters in general have been shown to export a wide range of substrate molecules, including lipids and hydrophobic compounds [19, 20]. Many lipophilic compounds conjugated with glutathione are substrates for the MRP family and the over-expression of MRP1 was shown to increase ATP-dependent glutathione S-conjugate

carrier activity, whereas MRP1 inhibitors diminish cellular extrusion of GSSG [14, 18, 21]. Therefore, members of this ubiquitous super family of ABC efflux pumps play a decisive role in cellular detoxification, stress response and defense against oxidative stress, constituting a first line of defense against environmental toxins [18].

As a lipophilic hydrophobic cation, farnesol classifies as a compound that conjugates with GSH, particularly given its known deleterious effect on cells [11]. Therefore, conjugation of farnesol with intracellular GSH, resulting in the disruption of the intracellular redox equilibrium, would provide a pathway ultimately leading to cellular apoptosis. In this current study, we aimed to demonstrate that the farnesol-induced apoptotic process in OSCCs involves alteration of cellular redox status through conjugation with reduced GSH, modulation of MRP1 induction, export of glutathione/farnesol S-conjugates (GS-F) and GSSG and disruption of the GSH/GSSG ratio, predisposing the cell to apoptosis.

MATERIALS AND METHODS

Reagents and cell cultures

Farnesol, MRP1 inhibitor (MK-571 sodium salt hydrate), reduced glutathione, 3-(4,5-dimethylthiazol-2-yl)-2,5-diphenyltetrazolium bromide and Glutathione Assay Kit were obtained from Sigma (Sigma-Aldrich Chemical, St. Louis, MO); QCRL-4 antibody from Santa Cruz Biotechnology (Santa Cruz Biotechnology, Santa Cruz, CA) and Lipodin-Ab from Abbiotec (Abbiotec, San Diego, CA). Farnesol was obtained as a 3 M stock solution and diluted to a 30 mM working stock solution in 100% methanol. Working stock solution was added to the culture media to required final concentration. Methanol was incorporated in the control experiments (0.2% final concentration) however, previous experiments had shown that methanol did not have an effect on cell viability at the concentration used in these experiments [22]. Glutathione (GSH) was reconstituted in distilled water to a final concentration of 20 mM and incorporated in experiments where indicated. Reduced glutathione had no significant effect on survival of control cells (data not shown). All experiments were performed using two established primary human tongue squamous cell carcinoma

cell lines (SCC9 and SCC25) from the American Type Culture Collection (Manassas, VA). Cells were cultured in 1:1 mix of Ham's F12 and Dulbecco's Modified Eagle's Medium (DMEM) (Invitrogen, Grand Island, NY) with 10% fetal bovine serum, 100 units of penicillin, 100 µg/ml streptomycin and 0.4 g/ml of hydrocortisone (Sigma-Aldrich). In some experiments glutamine-free DMEM media was used (Invitrogen, Grand Island, NY). The cells were cultured at 37 °C in a 5% CO₂ air atmosphere until confluent and sub-cultured using a disaggregation assay with trypsin (0.1%) and EDTA (0.01%) in phosphate buffered saline (PBS) of pH 7.5.

Farnesol treatment of OSCCs

Cells were grown in 75 cm² flask, 6- or 96-well plates at 2 x 10⁶, 6 x 10⁵ and 5 x 10⁴ cells per flask/well respectively, and grown to 80% confluence. Media was removed, cells were washed with PBS and fresh media was added with farnesol incorporated to final concentrations of 10, 20, 30, 45 and 60 µM. In order to determine the effect of farnesol on cells upon early and prolonged exposure, cells were treated with farnesol for 3 and 24 h. For all experiments, control cells were grown in media containing 0.2% methanol (vehicle for farnesol). All experiments were performed on three separate occasions.

MTS viability assay

Proliferation of farnesol-treated cells was assessed using the MTS Tetrazolium-Based Proliferation Assay (Promega, Madison, WI) according to manufacturer directions. Farnesol was added to the cells at final concentrations of 10, 20, 30, 45, 60 µM in the wells of a 96-well microtiter plate. Control reactions with cells and no farnesol were included. Plates were incubated for 3 or 24 h at 37 °C with 5% CO₂. Following incubation, media was aspirated, 200 µl PBS was added to each well with 20 µl of MTS reagent ([3-(4,5-dimethylthiazol-2-yl)-5-(3-carboxymethoxyphenyl)-2-(4-sulfophenyl)-2H-tetrazolium, inner salt]) and plates were incubated at 37 °C for 1 h 30 min or until color fully developed. Following color development, colorimetric change at 490 nm (A490) was measured with a microtiter plate reader (Titertrek, Multiskan MCC1340). In order to assess the effect of GSH supplementation on

cell viability, assays were also performed as described with GSH incorporated in the reactions at final concentration of 1 mM. Reactions on each occasion were performed in triplicate.

Light microscopy

Cells were grown on cover slips in 6-well plates at 6×10^5 cells per well and treated with farnesol as described above. Following 24 h incubation, cells were washed with 2 ml PBS, fixed in 4% formaldehyde for 15 min then washed three times with PBS. Coverslips were immediately mounted on slides and examined and imaged using a Leica microscope with digital image capture system.

Total cellular glutathione content

To determine whether farnesol impacts glutathione levels, the total cellular glutathione content was measured in farnesol-exposed cells using Glutathione Assay Kit (Sigma-Aldrich) according to manufacturer instructions. Briefly, cells were grown in 75 cm² flasks with farnesol for 3 or 24 h, harvested, washed with PBS and 3 volumes of 5% 5-Sulfosalicylic Acid (SSA) solution was added to the cell pellet. The suspension was frozen in liquid nitrogen and thawed in a 37 °C water bath then centrifuged at 10,000 x g for 10 min. Ten µl of supernatant was added to 150 µl working mixture for 5 min prior to addition of 50 µl NADPH. Absorbance at 412 nm was monitored at 1 min intervals for a total of 5 min. The content of total glutathione (nM/ml) was quantified by comparison with known glutathione standards.

Extracellular glutathione levels

In order to demonstrate the extracellular presence of glutathione mediated by farnesol, cells were grown in the presence and absence of farnesol for 3 and 24 h. Following incubation, cell-free spent media was collected and glutathione content was measured as described above. Experiments were also performed in growth media alone (no cells) in addition to a glutamine-free culture media to ensure lack of interference in glutathione measurement by media components.

Flow cytometry (apoptosis analysis)

In addition to MTS viability assays, the effect of farnesol on cell proliferation and apoptosis was evaluated using AnnexinV-Fluorescein isothiocyanate

(FITC) methods and flow cytometry as previously performed [11]. Briefly, following 3 or 24 h treatment with farnesol, cells were removed enzymatically, washed with media and cold PBS, and re-suspended in 1X binding buffer (BD-Pharmingen Biosciences, San Diego, CA). 5 µl of annexin V (apoptotic marker) and 5 µl propidium iodide (oncotic marker; Sigma-Aldrich) were added to cells, vortexed and incubated for 15 min in the dark. Following incubation, 400 µl of 1X binding buffer was added and samples were evaluated by flow cytometry and percent apoptosis determined from 3 separate experiments.

Scanning electron microscopy (SEM)

Farnesol-induced changes in cell morphology were assessed by SEM analysis, following 24 h exposure to farnesol, cells were washed twice with PBS then fixed in 2% paraformaldehyde and 2.5% glutaraldehyde in phosphate buffer, pH 7.4, for 1 h at room temperature, then 4 °C overnight. After initial fixation, specimens were washed in three changes of 0.1 M PBS for a total of 30 min, post-fixed with 1% osmium tetroxide in PBS for 1 h and washed again in three changes of buffer. Dehydration of specimens was done using a series of graded ethyl alcohol, 30%, 50%, 70%, 90% and 100%, for 10 min each and two more changes of 100% ethyl alcohol. Lastly, specimens were chemically dried by immersing sequentially in 2 parts 100% ethyl alcohol/1 part hexamethyldisilazane (HMDS) (Electron Microscopy Sciences, Fort Washington, PA) for 10 min, 1 part 100% ethyl alcohol/1 part HDMS for 10 min, 1 part 100% ethyl alcohol/2 parts HDMS for 10 min then 2 changes for 10 min each with 100% HDMS. Specimens were air dried in a hood overnight, mounted on SEM pin mounts and sputter coated with 10 to 20 nm of platinum/palladium in a sputter coater (EMS 150T ES). SEM images were captured in a scanning electron microscope Quanta 200 (FEI Co. Hillsboro, OR). Cells without farnesol were included as a control.

Confocal microscopy

In order to confirm the morphological changes in cells treated with farnesol, cells were grown on cover slips in 6-well plates at 6×10^5 cells per well then treated with farnesol (10, 30 and 60 µM) as described above. Following 3 h incubation, cells

were washed then stained with a mixture of 1 μ l/2 ml dichlorodihydrofluorescein diacetate (5 mM in EtOH; DCDHF-DA; Molecular Probes) for 30 min at room temperature in the dark. Cells were then washed twice with PBS and morphological changes assessed and imaged with a confocal fluorescent microscope Zeiss LSM 510 (Carl Zeiss, Thornwood, NY) and images captured using 60X and 100X oil-immersion objectives and a FITC filter.

Gene expression analysis

For detection of early expression of MRP1 gene induced by farnesol, the following gene-specific primer pairs (5'-3') were designed based on gene sequences in GenBank:

MRP1-B:AGGGCTCCATAGACGCTCAG;
MRP1-F:GCGCTGGCTTCCAACCTATTG;
GAPDH-F:TGGGCTACACTGAGCACCAG;
GAPDH-B:GGGTGTCGCTGTTGAAGTCA. Total RNA was extracted from cells using RNAqueous kit (Life Technologies, Carlsbad, CA) and DNA removed by RQ1 RNase-Free DNase (Promega, Madison, WI). The RNA concentration was determined using UV/VIS spectrophotometer. Absence of genomic DNA was confirmed by PCR using β -actin primers. Reverse transcription was performed using 2 μ g total RNA and Omniscript RT Kit (Qiagen, Valencia, CA) and real time PCR was performed using iTaq SYBR Green Supermix (Bio-Rad Labs, Hercules, CA) and ABI 7000 real time PCR machine (Applied Biosystems). Amplification was achieved using the following cycle settings: 30 s 95 °C followed by 40 cycles of 95 °C 15 s and 60 °C 1 min. Following amplification, a melt curve was analyzed to ensure the absence of primer dimers and expression was calculated using the $2^{-\Delta\Delta CT}$ method using GAPDH as reference gene.

Western blot

For MRP1 protein expression analysis, following treatment of cells with farnesol as described above, cells were washed twice with ice cold PBS and protein extracted using the M-PER Mammalian Protein Extraction Reagent (Thermo Fisher Scientific, Rockford, IL) per manufacturer recommendations. Protein concentration was measured and equalized using the Bio-Rad Protein Assay (Bio-Rad Labs, Richmond, CA). Electrophoresis was performed on 4-15% gradient polyacrylamide gels (Bio-Rad

Labs, Richmond, CA) followed by Western blotting using a 1:500 dilution of monoclonal primary antibody for MRP1 (Abcam, Cambridge, MA) with β -actin (Sigma-Aldrich) as a loading control. Blots were processed with Immobilon™ Western Chemiluminescent HRP Substrate (EMD Millipore Corporation, Billerica, MA) and imaged using HyBlot CL Autoradiography Film (Denville Scientific, South Plainfield, NJ).

Inhibition of MRP1 by MK571

In order to assess the impact of MRP1 inhibition on cell response to farnesol, viability assays were performed in the absence and presence of MK571, an LTD4 receptor antagonist and MRP1 inhibitor. MK571 was incorporated in farnesol-media mixture at final concentrations of 10 μ M for SCC25 and 30 μ M for SCC9. Control experiments were performed following the same procedure except without any farnesol in the solution. Viability was assessed using the MTS assay as described above.

QCRL-4 antibody blocking experiment

Similarly, to more specifically demonstrate the impact of MRP1 inhibition on cell viability an MRP1-specific monoclonal antibody was used. The following antibody transfection procedure was performed: 2 μ l of antibody solution (0.4 μ g) was mixed thoroughly with 0.1 μ l Lipodin-Ab solution and incubated for 15 min at room temperature. Following incubation 100 μ l of serum-free media was added to the antibody/Lipodin-Ab solution then immediately added to the cells. The cells were washed with 100 μ l serum-free media solution once before the antibody/Lipodin-Ab solution was added. Cells were then incubated for 5-6 h, washed twice with 200 μ l of buffer then new media added with farnesol incorporated to final concentrations of 30, 45, and 60 μ M. Reactions were incubated for 3 or 24 h and viability assessed using the MTS assay as described above. Control experiments were also performed to test the effect of the antibodies and Lipodin on cell viability.

Statistical analysis

For all measurements, a Student's t-Test was used to assess the statistical significance of treated groups versus control groups along with standard error. A statistically significant difference was considered to be present at p value of < 0.05.

RESULTS

MTS viability assay

Proliferation of cells exposed to increasing concentrations of farnesol was assessed by measuring absorbance following color development. Results indicated a significant killing effect for farnesol on both cell lines proportional to farnesol concentration and exposure time (Figure 1A). Although both cell lines were sensitive to farnesol, some differences in susceptibility were noted between the 2 cell lines with SCC9 demonstrating higher tolerance. However, the percent killing by farnesol was significantly reduced for both cell lines upon exogenous supplementation with GSH (Figure 1B). No killing for farnesol was noted at

concentrations below 30 μM and cells did not survive at concentrations above 60 μM .

Light microscopy

Proliferation of cells exposed to increasing concentrations of farnesol was assessed under optical light microscope. Consistent with results from the viability assay, images demonstrated a significant killing effect for farnesol on both cell lines proportional to farnesol concentration (Figure 2). Cells were seen undergoing morphological changes and sloughing off the surface at 30, 45 and 60 μM . In contrast, at low concentrations of farnesol (10, 20 μM), cell morphology and architecture remained unchanged in both cell lines.

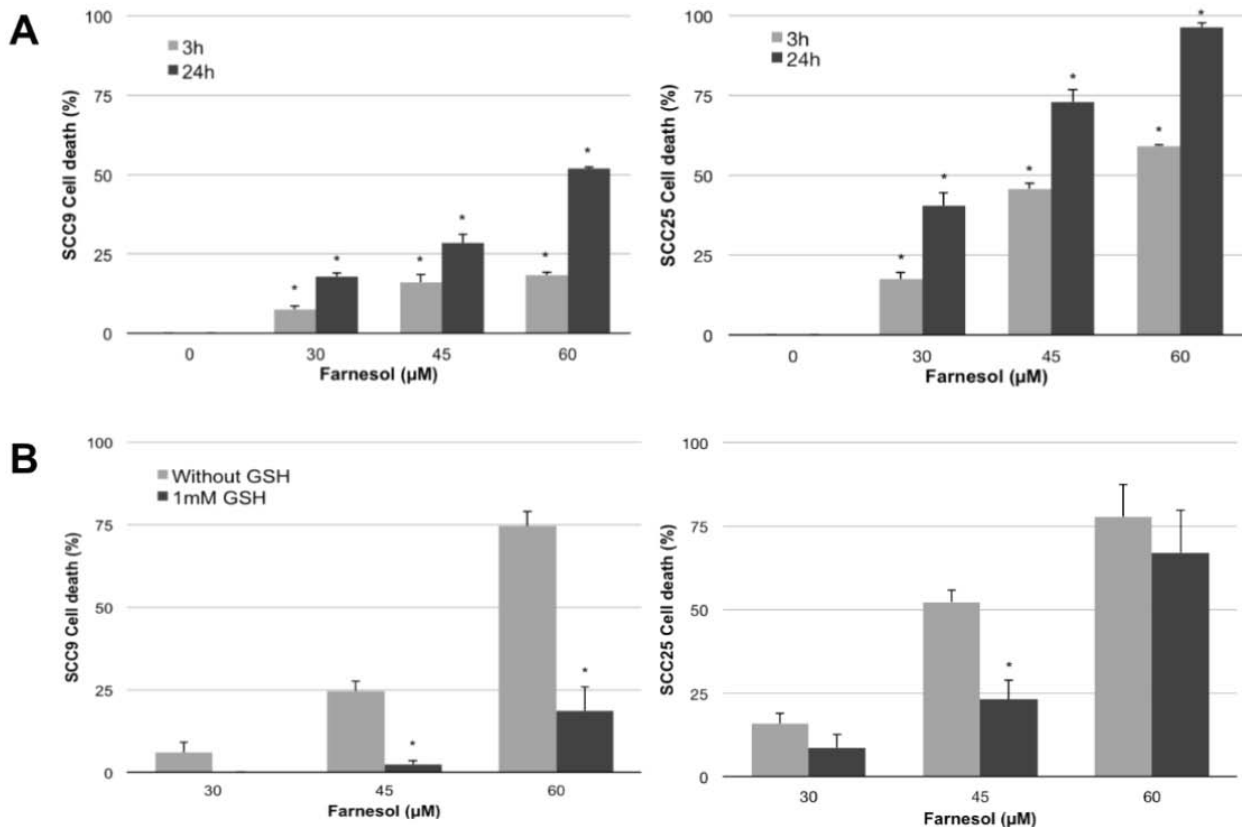


Figure 1. Farnesol concentration and exposure time-dependent killing of OSCCs and effect of GSH supplementation. Cell viability was assessed using the MTS metabolic assay. (A) Results demonstrated gradual increase in percent killing proportional to farnesol concentration and exposure time. The trend was the same for both cell lines, however cell line SCC9 exhibited higher tolerance to farnesol than SCC25. Cell viability as assessed using the MTS metabolic assay demonstrated the typical increase in percent killing proportional to farnesol concentration. (B) However, upon supplementation with exogenous glutathione (GSH), percent killing was significantly reduced at all farnesol concentrations tested. Interestingly, GSH seemed to be more effective in conferring tolerance to farnesol in SCC9 cell line compared to SCC25. Error bars indicate the standard errors of the means (* $p \leq 0.05$).

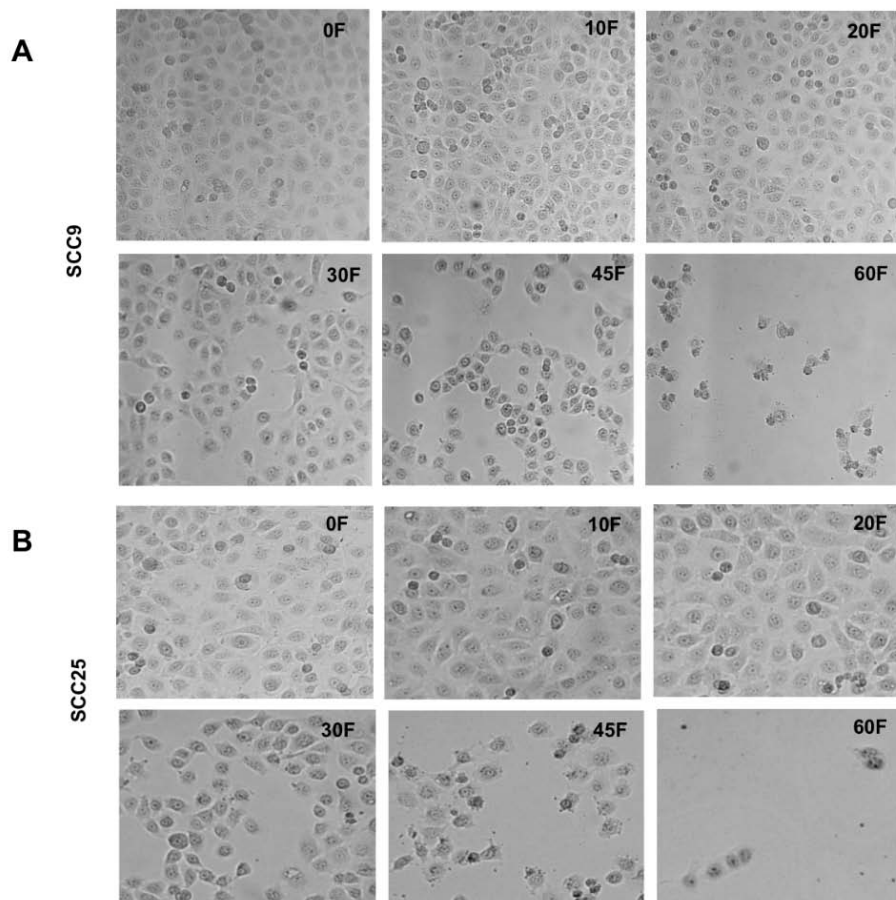


Figure 2. Light microscopy images of the two cell lines untreated or treated with increasing concentrations of farnesol for 24 h. Cells not exposed to farnesol or treated with concentrations below 30 μM (30F) exhibited normal morphology. In contrast, at 30 μM and above most cells in the farnesol-treated groups revealed characteristics such as rounding, shrinkage, and loss of contact with neighboring cells. In addition to the heterogeneous appearance, there was also a decrease in the number of cells which was more pronounced with increasing farnesol concentrations, with minimal cells seen attached in the cells treated with 60 μM (60F) (x40). Data represent of experiments performed in triplicate.

Total intracellular and extracellular glutathione content

To assess the impact of farnesol on glutathione levels, experiments were performed where both cells and spent culture media were harvested and recovered, respectively, and glutathione levels measured comparatively in control and farnesol-exposed cells. Results demonstrated a significant decrease in total cellular glutathione content proportional to farnesol concentration and time of exposure with a maximum drop noted at 60 μM for both cell lines (Figure 3A, B). The drop in intracellular levels was inversely proportional to those measured in the spent media under the same conditions where levels of extracellular glutathione

increased with increasing farnesol concentrations (Figure 3A, B). Interestingly, the baseline glutathione concentration (0F) was significantly higher at 24 h compared to 3 h. In addition, although the decrease in intracellular levels and concomitant increase in extracellular concentrations were comparable between the two cell lines at 3 h, SCC9 exhibited lower intracellular and higher extracellular levels at all farnesol concentrations, likely due to the lower baseline intracellular glutathione levels in this cell line.

Extracellular glutathione levels

In order to associate the decrease in intracellular glutathione levels with extrusion, the extracellular milieu was assessed for total glutathione following growth of cells in the presence of farnesol. Compared

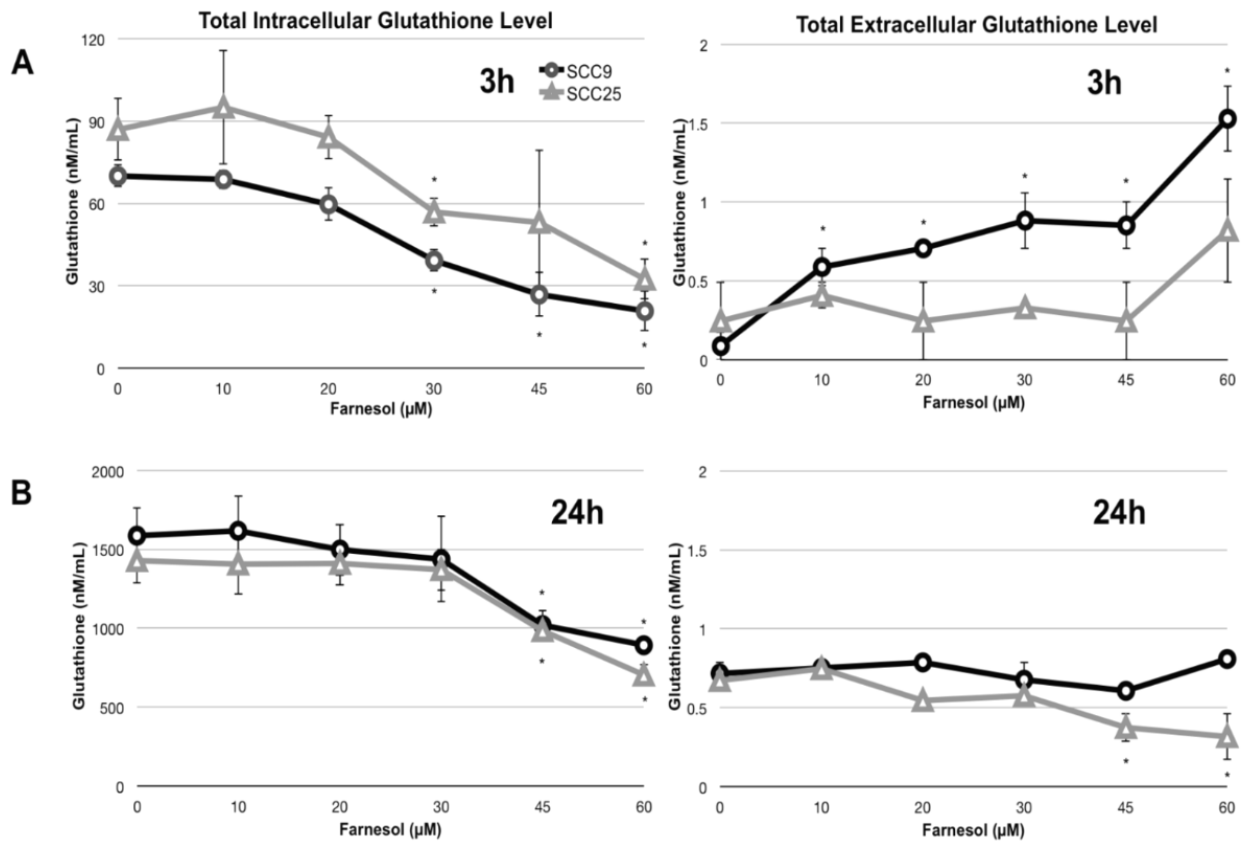


Figure 3. Effect of farnesol on intracellular and extracellular levels of glutathione following 3 and 24 h exposure to increasing farnesol concentrations. Cells of both cell lines were harvested, lysed and intracellular glutathione levels were measured using the glutathione assay kit. Spent growth media was also collected, clarified and glutathione was similarly quantified in the supernatant. Significant decrease in intracellular glutathione levels was seen in both cell lines proportional to farnesol concentration and exposure time. The drop in intracellular levels was concomitant with increase in level of detection of total glutathione in the extracellular growth milieu. Although at 3 h (A) a more significant drop in levels was seen in SCC25 cells, no significant differences between the cell lines was noted at 24 h (B). Of note, in cells not exposed to farnesol (0F), the baseline intracellular glutathione levels for both cell lines was significantly higher in 24 h-old cells compared to 3 h indicating cell age-dependent changes in GSH levels. Error bars indicate the standard errors of the means (* $p \leq 0.05$).

to control experiments (no farnesol), results from these experiments demonstrated a gradual increase in total glutathione levels in the media proportional to farnesol concentration following 3 h treatment, with higher levels detected for the SCC9 cell line compared to SCC25 (Figure 3A). However, no significant changes in extracellular glutathione levels were noted following 24 h treatment with farnesol (Figure 3B).

Flow cytometry (apoptosis analysis)

The apoptotic effect of farnesol on the cells was corroborated by results from flow cytometry following Annexin V and Propidium iodide (PI) staining.

Consistent with viability assays, results demonstrated a concentration-dependent increase in annexin V labeling and PI staining, with a maximal increase at 60 μM (Figure 4).

Scanning electron microscopy (SEM)

Farnesol-induced morphological changes in cells were assessed by SEM. Results indicated a significant effect of farnesol proportional to farnesol concentration. At 30 μM cells were seen undergoing apoptosis with cytosol condensation and blebbing phenomenon, which characterize apoptotic cell death. At higher farnesol concentration (60 μM) cells appeared necrotic exhibiting features such as rupture of the cytoplasmic

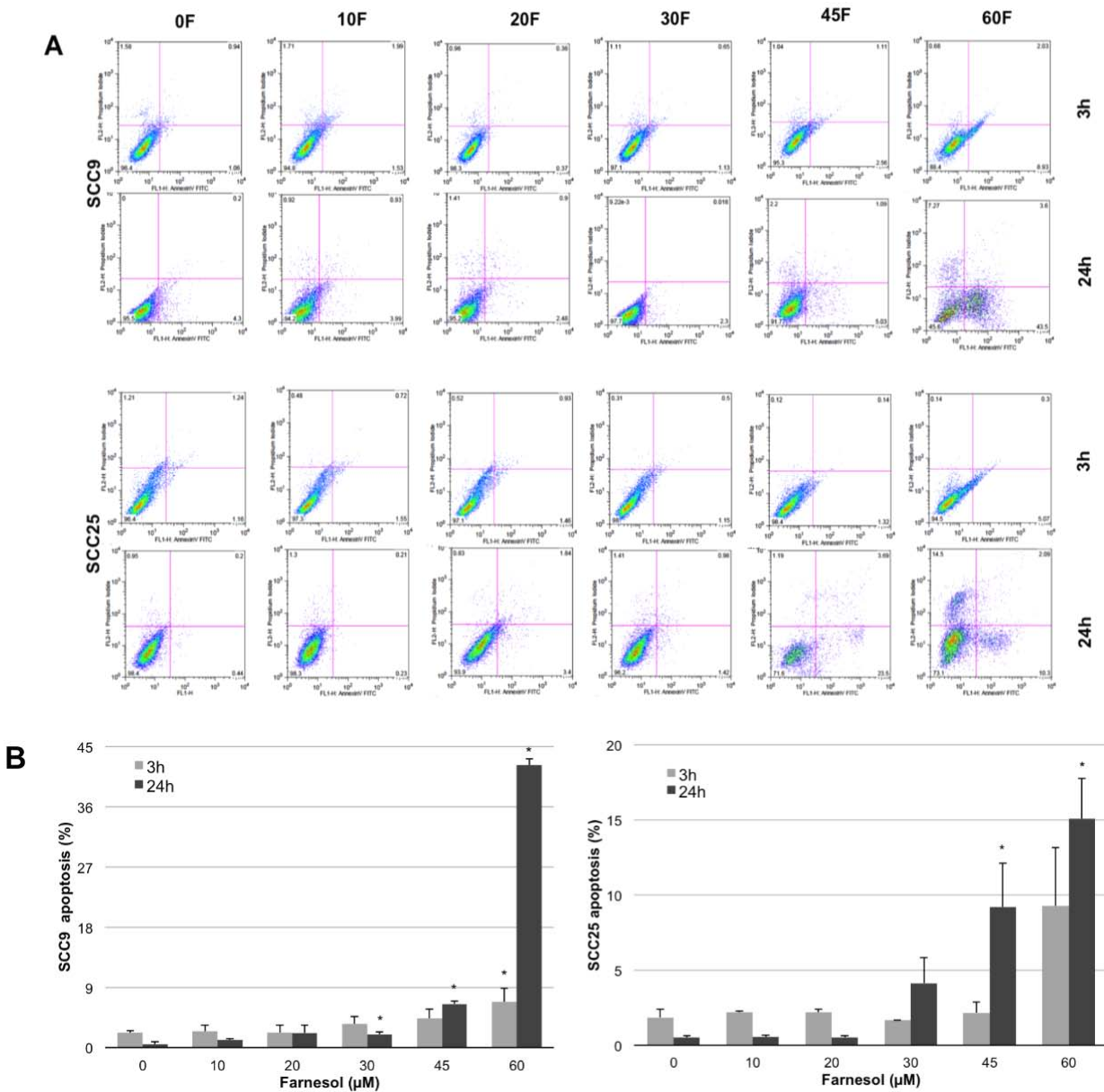


Figure 4. Effect of farnesol on Annexin V and PI binding. Representative flow cytometry graphs of cells treated with different concentrations of farnesol. Cells isolated and prepared for measurement of Annexin V and PI staining using flow cytometry analysis in order to count the number of cells that have undergone apoptosis. (A) Contour plots with quadrant gates show four populations; in the untreated control sample, the majority (%) of cells were viable and non-apoptotic (Annexin V⁻/PI⁻). However, with increasing concentrations of farnesol, there was a decrease in the population and an increase in cells undergoing early apoptosis (Annexin V⁺/PI⁻). An increase in the Annexin V⁺/PI⁺ population indicating dead or necrotic cells was observed at higher doses of farnesol. Percent apoptosis for both cell lines were also shown in graph (B).

membrane with preserved cell center (nucleus). However, at low concentration of farnesol (10 μM), cell morphology and architecture remained unchanged and comparable to control cells (Figure 5A,B).

Confocal microscopy

Morphological changes of cells were also assessed using confocal microscopy. Images revealed a significant effect for farnesol proportional

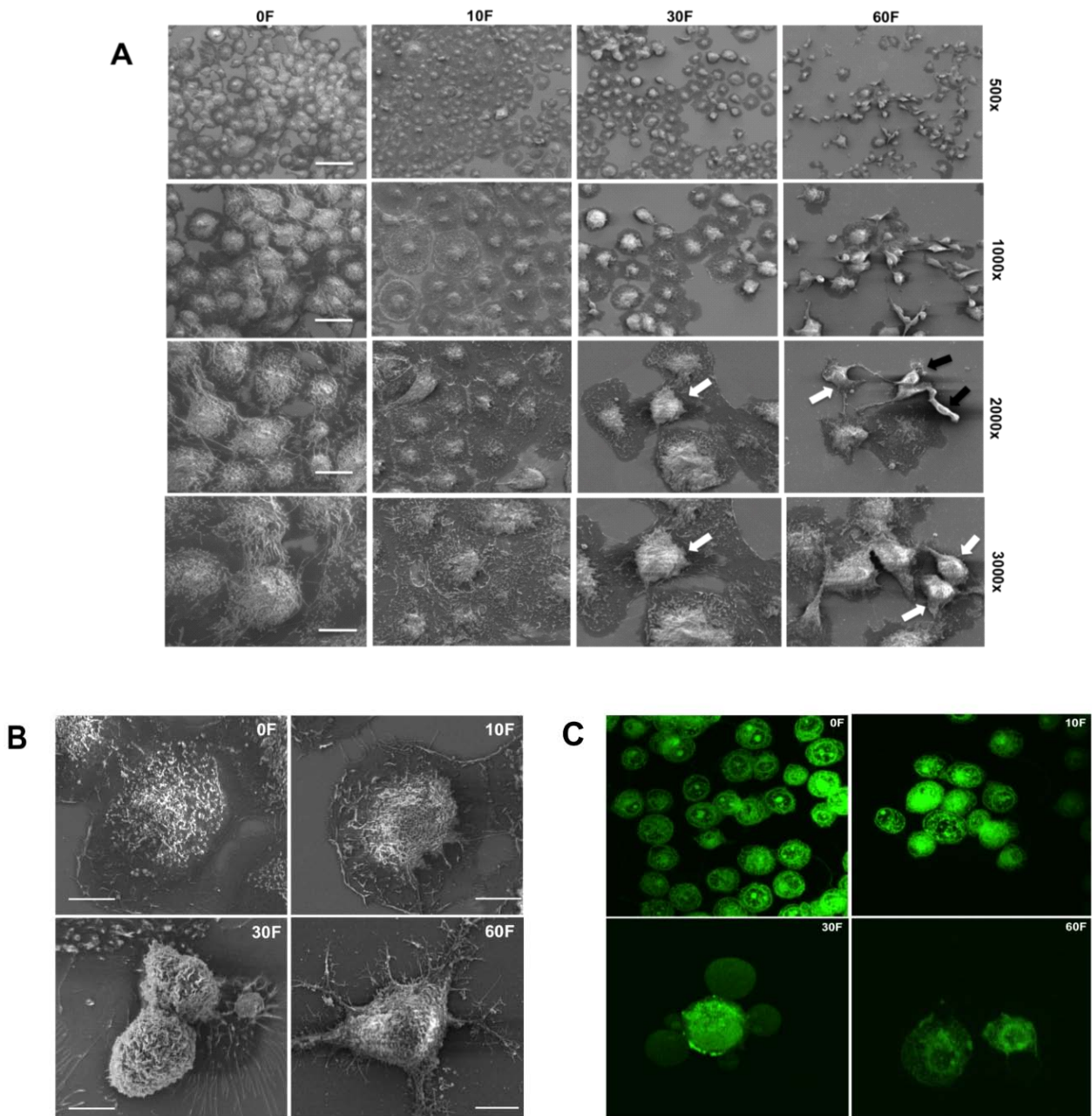


Figure 5. Representative microscopic confocal fluorescent and scanning electron images of farnesol-treated cells demonstrating the sequence of the apoptotic process induced by farnesol in SCC25 cells.

(A) SEM analysis demonstrated no morphological changes in cells at 0F and 10 μ M (10F). However, apoptotic cells (white arrows) were detected at 30 μ M (30F) with characteristic surface blebs (apoptotic bodies). Necrotic cells (black arrows) were seen mostly at 60 μ M (60F) demonstrating rounded morphology with ruptured cytoplasm. Scale bars represent (A) 200, 100, 50 and 30 μ m for 500, 1000, 2000 and 3000x magnification, respectively, and 20 μ m for 5000x magnification in (B). (C) Cells treated with farnesol were also incubated with dichlorodihydrofluorescein diacetate (green fluorescence) and the various phases of apoptosis were visualized by confocal laser scanning microscopy. Morphological changes in cell membrane can be seen at higher farnesol concentrations followed by formation of cell surface blebbing, cell fragmentation and apoptotic bodies, suggestive of cell death via apoptotic pathway.

to concentration. Cells were seen undergoing changes consistent with apoptotic death at 30 μM farnesol including changes in the nucleus followed by plasma membrane, cytosol condensation and blebbing, phenomenon characterizing apoptotic cell death. At 60 μM , early stage of secondary necrosis as an outcome of complete apoptosis was seen in cells that have gone through apoptotic alterations, exhibiting necrotic features such as rupture of the cytoplasmic membrane and nuclear deterioration. Consistent with viability assays, at low concentration of farnesol (10 μM), cell morphology and architecture was seemingly unchanged, resembling that of control cells. Representative images are shown (Figure 5C).

MRP1 gene expression

Gene expression studies using qRT-PCR were performed in order to determine whether farnesol exposure modulates the expression of the MRP1 efflux pump. Results from these experiments demonstrated that farnesol exposure induced significant increase in the expression of MRP1 relative to the untreated control cells in both cell lines (Figure 6A). However, the fold increase in expression differed between the cell lines at some farnesol concentrations with SCC9 demonstrating a gradual increase proportional to farnesol concentration with the highest levels detected at 30 μM . In contrast, in SCC25 although levels increased at 20 μM , expression dropped at 30 μM .

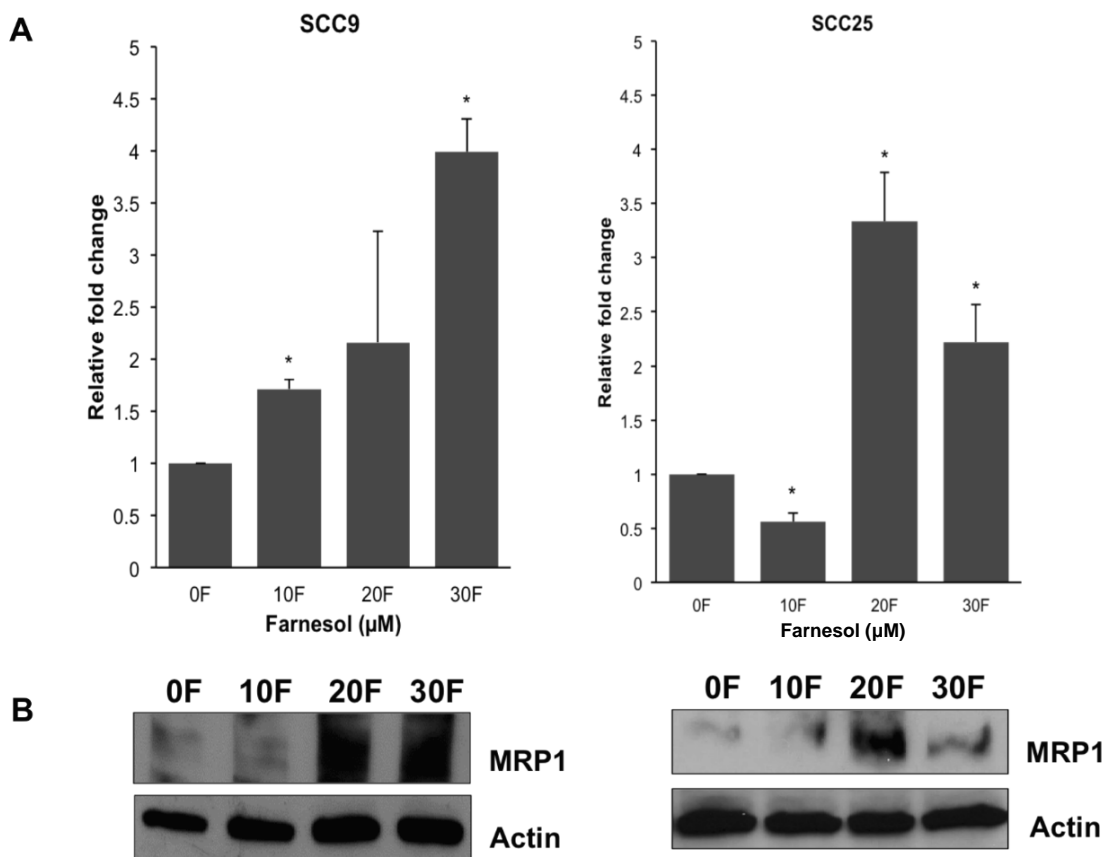


Figure 6. Effect of farnesol on early gene and protein expression of MRP1 in SCC9 and SCC25 cells following 3 h exposure to increasing concentrations of farnesol. (A) qRT-PCR analysis demonstrated significant increase in MRP1 expression relative to the untreated control cells with differences in gene expression noted between the two cell lines. Data represents the average of 3 independent experiments performed in triplicate. Error bars indicate the standard errors of the means (* $p \leq 0.05$). (B) Similarly, Western blot analysis demonstrated significant up-regulation of MRP1 proportional to farnesol concentration consistent with gene expression profiles. Beta Actin was used as loading control. MRP1 band typically appears dispersed and not well defined as previously demonstrated [27-31].

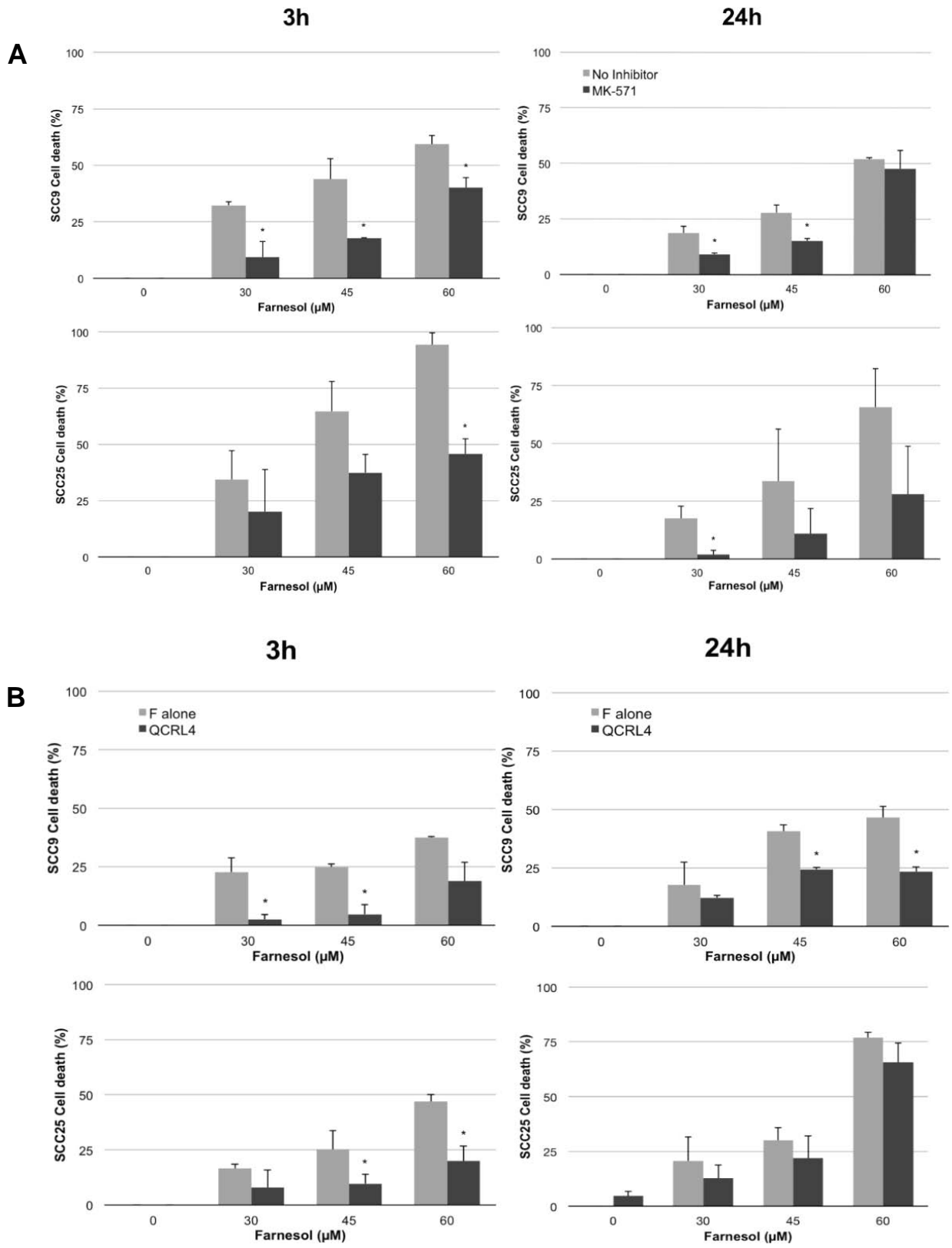


Figure 7

Since farnesol exerts a significant killing effect at concentrations higher than 30 μ M, not enough cells could be harvested for MRP1 expression studies.

Western blot analysis

Proteins extracted from cells were subjected to SDS-PAGE and membranes were probed with antibodies to MRP1. Protein expression profiles demonstrated a significant increase in the expression of MRP1 proportional to farnesol concentration (Figure 6B). Interestingly, in SCC25, higher levels of MRP1 were seen at 20 μ M than 30 μ M, consistent with gene expression levels.

Effect of MRP1 inhibition on cell viability

In order to validate the hypothesis that the effect of farnesol on cell viability is associated with MRP1 activity, viability assays were performed in the presence of MK-571, a first class inhibitor of MRP1. Results from these assays demonstrated a significant decrease in percent killing of farnesol at both time points in the presence of the inhibitor with a more drastic effect seen on the SCC25 cell line (Figure 7A).

Selective inhibition of MRP1 by QCRL-4 monoclonal antibody

In addition to inhibition by the MK-571 inhibitor, specific antibody blocking of MRP1 was also performed. The QCRL-4 antibody can be used to selectively block the MRP1 pump in live cells. Consistent with the results from MK-571, transfection of monoclonal antibody significantly reduced killing by farnesol at all concentrations, both time points and in both cell lines. In general, the antibody seemed to have a more pronounced effect on SCC9 (Figure 7B). Lipodin, QCRL4 and IgG were tested for effect on cell viability. No additional loss in viability was observed beyond

what was seen for non-transfected cells treated with farnesol alone.

DISCUSSION

Apoptosis is a naturally occurring developmental process triggered by various extracellular and intracellular stimuli [4, 5]. Although the exact mechanism of its cytotoxicity leading to apoptosis is yet to be elucidated, farnesol was recently identified as an extracellular stimulus of apoptosis in several human tumor cells, which now includes OSCCs [1, 11]. The current study was undertaken in order to validate the hypothesis that similar to the effect on fungal cells, farnesol toxicity in OSCCs involves oxidative stress mediated by intracellular glutathione consumption, extrusion and depletion.

Because of its hydrophobicity, farnesol can penetrate intact cell membranes and induce oxidative stress by producing superoxide and hydroxyl radicals. As part of the cell's defense against oxidative stress, GSH present inside the cell conjugates with farnesol forming GS-F conjugates. However, the conjugate retains the ability to carry out redox recycling to form superoxide and hydroxyl radicals, and therefore this by itself is not an effective detoxification pathway unless the conjugate is recognized by a membrane transporter as a substrate and pumped out of the cell by an ATP-driven process. In combination, these two cellular strategies indicate the presence of a coordinated antioxidant cellular response. In this study, a farnesol-induced cellular stress was demonstrated by flow cytometry analysis where cells were seen undergoing various stages of apoptosis proportional to farnesol concentration.

Further, the involvement of GSH in the cytotoxic process was clearly demonstrated by the decrease in its intracellular levels concomitant with decrease in cell viability, which was alleviated

Legend to Figure 7. Effect of inhibition of MRP1 on cell viability in response to farnesol using the MK-571 specific inhibitor of MRP1 and MRP1-specific antibody. (A) In the presence of an MRP inhibitor, a significant decrease in percent killing was seen in farnesol-treated cells in the presence of the inhibitor compared to treated cells without inhibitor at both time points, with more pronounced effect noted on SCC25. (B) The QCRL-4 antibody was used to selectively block MRP1. When delivered inside the cell, the antibody binds to its specific epitope preventing the MRP1 pump from changing its configuration, thus stopping any transport. Similar to results with MK-571 inhibitor, a significant decrease in farnesol killing was seen in both cell lines and time points at all farnesol concentrations tested with more pronounced effect noted on SCC9 compared to SCC25 (* $p \leq 0.05$).

upon exogenous supplementation of GSH. Importantly, the reduced intracellular levels upon exposure to farnesol paralleled an increase in detectable levels of extracellular glutathione, indicating extrusion of oxidized and/or conjugated glutathione from the cell. These findings are in line with those from a recent study by Koley *et al.* [22] investigating oxidative stress induced in HeLa cells by menadione, a cytotoxic hydrophobic molecule similar to farnesol. Since thiodione is known to be the resulting conjugate between menadione and GSH, the authors were able to quantitatively estimate the MRP1-mediated thiodione efflux from the cell. In our case however, farnesol conjugation with GSH was not previously demonstrated and therefore, the identity and stability of formed farnesol-GSH conjugates is not known, which made it problematic to measure their intracellular and extracellular levels.

In order to validate the hypothesis that lack of MRP1 as a transporter enhances survival of cells in the presence of farnesol, MRP1 specific inhibition studies were performed using a chemical inhibitor and cell transfection by a specific monoclonal antibody. Results from these experiments demonstrated a marked effect on OSCC cell survival upon MRP1 inhibition. Interestingly, these findings are paradoxical as the overexpression of ABC transporters typically constitutes a mechanism by which the cell develops resistance to chemotherapeutic agents. However, the induction of these transporters by farnesol-GSH conjugates and GSSG serving as an immediate mechanism for the cell to rid itself of oxidized species paradoxically disrupts the cellular redox balance and cell function. Therefore, inhibition of these transporters allows the cell to recycle conjugated GSH and reduce GSSG thereby maintaining sufficient levels of total intracellular GSH and in turn redox potential promoting cell survival and function.

It is important to note however, that the hydrophobic nature of farnesol favors its accumulation in cell membranes, which could result in disruption of membrane integrity, as we have previously demonstrated in microbial cells [23, 24]. Therefore, at high concentrations and prolonged exposure, it is likely that farnesol

causes extensive disruption of the cell membrane leading to immediate cell death or necrosis. However, at early time points of exposure and lower concentrations, farnesol toxicity is mediated by rapid disruption of GSH levels as shown by our findings. In combination, these two mechanisms indicate the simultaneous induction of apoptosis and necrosis as demonstrated by flow cytometry and fluorescent microscopy.

Although the response of both cell lines used in this study to farnesol was comparable and consistent in all experiments performed, some differences were seen in terms of level of response where, in general, SCC9 seemingly exhibited higher tolerance to farnesol. Intrinsic differences between cell lines are expected particularly in cancer cells derived from patients with varying clinical disease progression. Interestingly, on comparing the properties of the two cell lines based on the analysis of our results, SCC9 exhibited higher MRP1 protein expression and GSH supplementation seemed to be more effective in conferring tolerance to this cell line. Whether these observations explicate some of the observed differences in response to farnesol however, is unclear. Another interesting observation is that the baseline intracellular GSH levels in both cell lines regardless of farnesol (0F) was significantly higher in cells grown for 24 h compared to 3 h. This is expected as age-associated oxidative stress increases the demand for GSH and in turn, its *de novo* synthesis as a compensatory mechanism.

Farnesol concentrations below 20 μ M did not exhibit a noticeable adverse effect on the cells. These observations are interesting since farnesol is an intermediate in the sterol biosynthesis pathway in eukaryotic cells normally present in the cell at low concentrations. Therefore, it is conceivable that farnesol may play an important physiological role in the eukaryotic cell whereby by exerting a low level of stress it induces a response by the cell as a self-defense mechanism, which may benefit the cell in stressful conditions such as in the presence of chemotherapeutic agents. In that sense, farnesol may be a key component in the cell's resistance mechanism to anti-cancer drugs. Interestingly and along those lines, a recent study by Tai *et al.* [25] indicated that intracellular redox status may be closely

correlated with multidrug resistance in gastric adenocarcinoma cells. Further, given the establishment of a farnesol-induced cellular apoptotic process, it is tempting to speculate that through the regulation of intracellular farnesol production, eukaryotic cells may have developed a mechanism of altruistic programmed cell death with evolutionary advantages [26]. These inferences however, require in depth investigations where intracellular levels of farnesol are measured and analyzed under different conditions and stages of the cell life cycle.

CONCLUSION

In conclusion, xenobiotics induce cytotoxicity by different pathways; a redox recycler exerts oxidative stress by forming ROS and GSSG thus, depleting intracellular GSH. Alternatively, a second type of xenobiotic, an arylator, depletes intracellular GSH through the formation of GS-conjugates (arylation). Here, we present novel findings indicating that farnesol can act as both a redox cyler and arylator. To our knowledge, this is the first study elucidating a defined mechanism behind farnesol-induced apoptosis in human tumor cells. We expect the findings to pave the way for more in depth investigations to enable a better understanding of the molecular mechanisms underlying farnesol-mediated cytotoxicity in eukaryotic cells. Significantly, studies are warranted to explore the potential of this redox-cycling agent as an alternative anti-tumor agent.

ACKNOWLEDGEMENTS

We would like to thank the University of Maryland Core Imaging Facility for assistance with electron microscopy. This work was supported by the National Institute of Health grant DE016257 NIH/NAID and the Interuniversity Attraction Poles Programme initiated by the Belgian Science Policy Office.

CONFLICT OF INTEREST STATEMENT

No conflict of interest.

REFERENCES

1. Wright, M. M. and McMaster, C. R. 2002, *Biol. Res.*, 35, 223-229.

2. Lo, M. L., Pannone, G., Staibano, S., Mignogna, M. D., Rubini, C., Mariggio, M. A., Procaccini, M., Ferrari, F., De Rosa, G. and Altieri, D. C. 2003, *Br. J. Cancer*, 89, 2244-2248.
3. Parkin, D. M., Bray, F., Ferlay, J. and Pisani, P. 2005, *CA Cancer J. Clin.*, 55, 74-108.
4. Enari, M., Sakahira, H., Yokoyama, H., Okawa, K., Iwamatsu, A. and Nagata, S. 1998, *Nature*, 391, 43-50.
5. Hengartner, M. O. 2001, *Nature*, 412, 27-29.
6. Burke, Y. D., Ayoubi, A. S., Werner, S. R., McFarland, B. C., Heilman, D. K., Ruggeri, B. A. and Crowell, P. L. 2002, *Anticancer Res.*, 22, 3127-3134.
7. Rao, C. V., Newmark, H. L. and Reddy, B. S. 2002, *Cancer Detect. Prev.*, 26, 419-425.
8. Wiseman, D. A., Werner, S. R. and Crowell, P. L. 2006, *J. Pharmacol. Exper. Ther.*, 320, 1163-1170.
9. Voziyan, P. A., Haug, J. S. and Melnykovych, G. 1995, *Biochem. Biophys. Res. Commun.*, 212, 479-486.
10. Edwards, P. A. and Ericsson, J. 1999, *Annu. Rev. Biochem.*, 68, 157-185.
11. Scheper, M. A., Shirliff, M. E., Meiller, T. F., Peters, B. and Jabra-Rizk, M. A. 2008, *Neoplasia.*, 10, 954-963.
12. Dickinson, D. A. and Forman, H. J. 2002, *Ann. NY Acad. Sci.*, 973, 488-504.
13. Pastore, A., Federici, G., Bertini, E. and Piemonte, F. 2003, *Clin. Chim. Acta*, 333, 19-39.
14. Trompier, D., Chang, X-B., Barattin, R., d'Hardemare, A. M., Di Pietro, A. and Baubichon-Cortay, H. 2004, *Cancer Res.*, 64, 4950-4956.
15. Penninckx, M. J. 2002, *FEMS Yeast. Res.*, 2, 295-305.
16. Baek, Y-U., Kim, Y-R., Yim, H-S. and Kang, S-O. 2004, *FEBS Lett.*, 556, 47-52.
17. Grant, C. M., Collinson, L. P., Roe, J-H. and Dawes, I. W. 1996, *Mol. Microbiol.*, 21, 171-179.
18. Kruh, G. D. and Belinsky, M. G. 2003, *Oncogene*, 22, 7537-7552.
19. Toyoda, Y., Hagiya, Y., Adachi, T., Hoshijima, K., Kuo, M. T. and Ishikawa, T. 2008, *Xenobiotica*, 38, 833-862.

20. Rappa, G., Lorico, A., Flavell, R. A. and Sartorelli, A. C. 1997, *Cancer Res.*, 57, 5232-5237.
21. Lorico, A., Rappa, G., Finch, R. A., Yang, D., Flavell, R. A. and Sartorelli, A. C. 1997, *Cancer Res.*, 57, 5238-5242.
22. Koley, D. and Bard, A. J. 2012, *Proc. Nat. Acad. Sci. USA*, 109, 11522-11527.
23. White, T. C., Marr, K. A. and Bowden, R. A. 1998, *Clin. Microbiol. Rev.*, 11, 382-402.
24. Jabra-Rizk, M. A., Meiller, T. F., James, C. and Shirliff, M. E. 2006, *Antimicrob. Agents Chemother.*, 50, 1463-1469.
25. Tai, D-J., Jin, W-S., Wu, G-S., Si, H-W., Cao, X-D., Guo, A-J. and Chang, J-C. 2012, *Exp. Ther. Med.*, 4, 291-296.
26. Dawson, C., Intapa, C. and Jabra-Rizk, M. A. 2011, *PLoS Pathog.*, doi:10.1371/journal.ppat.1002121.
27. Juuti-Uusitalo, K., Vaajasaari, H., Ryhänen, T., Narkilahti, S., Suuronen, R., Mannermaa, E., Kaarniranta, K. and Skottman, H. 2012, *PLoS One*, doi:10.1371/journal.pone.0030089.
28. Krishnamachary, N., Ma, L., Zheng, L., Safa, A. R. and Center, M. S. 1993, *Oncol. Res.*, 6, 119-127.
29. Scheffer, G. L., Kool, M., Heijn, M., de Haas, M., Pijnenborg, A. C., Wijnholds, J., van Helvoort, A., de Jong, M. C., Hooijberg, J. H. and Mol, C. A. 2000, *Cancer Res.*, 60, 5269-5277.
30. Mao, Q., Qiu, W., Weigl, K. E., Lander, P. A., Tabas, L. B., Shepard, R. L., Dantzig, A. H., Deeley, R. G. and Cole, S. P. 2002, *J. Biol. Chem.*, 277, 28690-28699.
31. Rothnie, A., Conseil, G., Lau, A. Y., Deeley, R. G. and Cole, S. P. 2008, *Mol. Pharmacol.*, 74, 1630-1640.